

Evaluating geometrically-approximated principal component analysis vs. classical eigenfaces: a quantitative study using image quality metrics

Faouzia Ennaama¹, Sara Ennaama², Sana Chakri¹

¹Laboratory of Mathematics, Computer Science, Electrical Engineering and Physics (LAMIGEP), Moroccan School of Engineering Sciences (EMSI-Marrakesh), Marrakesh, Morocco

²SIGL Lab., National School of Applied Sciences (ENSA), Abdelmalek Essaadi University, Tetouan, Morocco

Article Info

Article history:

Received Jun 28, 2024

Revised Aug 24, 2024

Accepted Sep 3, 2024

Keywords:

Mean absolute error

Peak signal-to-noise ratio

Principal component analysis approximation

Signal-to-noise ratio

Structural similarity

ABSTRACT

Principal component analysis (PCA) is essential for diminishing the number of dimensions across various fields, preserving data integrity while simplifying complexity. Eigenfaces, a notable application of PCA, illustrates the method's effectiveness in facial recognition. This paper introduces a novel PCA approximation technique based on maximizing distance and compares it with the traditional eigenfaces approach. We employ several image quality metrics including Euclidean distance, mean absolute error (MAE), peak signal-to-noise ratio (PSNR), signal-to-noise ratio (SNR), and structural similarity index measure (SSIM) for a quantitative assessment. Experiments conducted on the Brazilian FEI database reveal significant differences between the approximated and classical eigenfaces. Despite these differences, our approximation method demonstrates superior performance in retrieval and search tasks, offering faster and parallelizable implementation. The results underscore the practical advantages of our approach, particularly in scenarios requiring rapid processing and expansion capabilities.

This is an open access article under the [CC BY-SA](https://creativecommons.org/licenses/by-sa/4.0/) license.



Corresponding Author:

Faouzia Ennaama

Laboratory of Mathematics, Computer Science, Electrical Engineering and Physics, Moroccan School of Engineering Sciences (EMSI-Marrakesh)

Marrakesh, Morocco

Email: faouzia.ennaama@ced.uca.ma

1. INTRODUCTION

Principal component analysis, commonly known as principal component analysis (PCA), is a powerful and well-established multivariate statistical technique employed in pattern recognition, computer vision, and signal processing. Initially introduced by Pearson in 1901 and later refined by Hotelling in 1933, PCA, sometimes referred to as the discrete Karhunen-Loève transformation [1]–[3], is designed to extract essential information from multivariate data by mapping the original high-dimensional space into a reduced-dimensional space. This process involves creating components that are linear combinations of the observed variables, effectively capturing the majority of the data's variability.

In 1991, Turk and Pentland [4] applied PCA to facial recognition, pioneering the eigenfaces method. This approach involves deriving facial features and representing them as a linear combination of "eigenfaces," which are eigenvectors obtained from the covariance matrix of the high-dimensional facial image space. The number of eigenfaces corresponds to the quantity of training images, and each face is then mapped into this reduced-dimensional space to determine the contribution of each eigenvector.

Although the eigenfaces method is effective for a limited number of low-resolution images, but it becomes less efficient as the dataset grows. The processing time increases, leading to longer training periods and higher computational costs. Recent advancements in integrated circuits and microelectronics, such as central processing units (CPUs), graphics processing units (GPUs), and field programmable gate array (FPGAs), have facilitated parallelization techniques [5], [6], significantly accelerating computations. The use of GPUs, in particular, has demonstrated substantial speed-ups in eigenfaces and PCA applications through parallel processing [7]–[9]. Compute unified device architecture (CUDA) implementations, for example, have been used to enhance the performance of these methods [10]–[16], enabling rapid and efficient processing.

In this paper, we propose an enhancement to the existing geometrical approximation of PCA, previously validated on synthetic 2D data with Gaussian distribution and effective for hyperspectral satellite image visualization. We compare this geometrically-approximated PCA method with the classical eigenfaces approach. To evaluate the effectiveness of both methods, we employ several quality metrics: Euclidean distance, peak signal-to-noise ratio (PSNR), mean absolute error (MAE), signal-to-noise ratio (SNR), and structural similarity index measure (SSIM). The results of this comparative study are detailed in section 4, with conclusions provided in the final section.

2. METHOD

The eigenfaces method [4] is a widely recognized technique in facial recognition and image processing. It transforms facial images into a set of characteristic features, known as eigenfaces, which represent the principal components of the image dataset. This technique employs PCA to identify the key features that account for the variance in facial images, facilitating effective recognition and comparison. Conversely, the approximate approach to eigenfaces simplifies and accelerates this process by using geometric approximations rather than traditional PCA computations. This approach focuses on identifying key eigenvectors based on geometric properties, such as the maximum distances between images in the dataset, potentially offering faster computation times while maintaining reasonable accuracy. Both methods aim to achieve reliable face recognition but differ in their underlying principles and computational strategies. The following sections detail these methods, exploring their methodologies, advantages, and limitations.

2.1. Eigenface approach

The eigenfaces technique, introduced by Turk and Pentland [4], is a classic technique for face recognition. It represents faces as linear combinations of “eigenfaces,” which are principal components generated from the collection of training face images. The key stages of the eigenfaces approach are outlined:

- a. Gather face images I_1, I_2, \dots, I_M as the training dataset. Ensure these images are standardized to have identical dimensions $N \times N$ and consistent lighting conditions.
- b. Convert the training images from RGB color space to grayscale.
- c. Transform images into vectors $\Gamma = \Gamma_1, \Gamma_2, \dots, \Gamma_M$: Convert image I to vector Γ_i with dimensions $N^2 \times 1$.
- d. Calculate the average face image Ψ :

$$\Psi = \frac{1}{M} \sum_{i=1}^M \Gamma_i \quad (1)$$

here, M denotes the overall count of images, and Γ_i corresponds to the vector representation of each image.

- e. Remove the average face from every face in the training dataset to obtain a set of different faces.

$$\Phi_i = \Gamma_i - \Psi \quad (2)$$

In this context, i ranges from 1 to M , and A is an $N^2 \times M$ matrix composed of $[\Phi_1, \Phi_2, \dots, \Phi_M]$.

- f. Obtain the covariance matrix from the difference faces.

$$C = \frac{1}{M} \sum_{i=1}^M \Phi_i \Phi_i^T = \frac{AA^T}{M} \quad (3)$$

where A^T denotes the transposition of the matrix constructed from $[\Phi_1, \Phi_2, \dots, \Phi_M]$

- g. Determine the principal elements (which are also known as eigenvectors) and their corresponding eigenvalues from the covariance matrix. The eigenfaces represent the primary components derived from the set of face images.

- h. Obtain the eigenfaces. Select the top K eigenvectors to form the eigenfaces.

$$\omega K = eT(\Gamma i - \Psi) \quad (4)$$

where K ranges from 1 to M' and indicates the count of chosen eigenvectors.

- i. Generate the weight vectors:

$$\Omega_K^T = [\omega_1, \omega_2, \dots, \omega_K] \quad (5)$$

- j. Use Euclidean distance to compare weight vectors:

$$\varepsilon_2 = \|\Omega - \Omega_k\|^2 \quad (6)$$

here, Ω_k denotes the vector that characterizes the K_{th} face class. A face is considered 'known' if the smallest ε_k falls below a specified threshold θ_ε ; otherwise, the face is classified as 'unknown'.

2.2. Classical approach

In this section, we revisit the geometrical approximation of PCA proposed by [17]. This method estimates eigenfaces for a dataset of face images based on the observation that the direction given by the furthest points in a multivariate dataset is often close to the first principal component, depending on data correlation. This approach is particularly effective in cases where the dataset exhibits strong correlations among variables, allowing the method to capture the most significant variance.

The method involves several steps. Firstly, the training set of face images is organized as a grayscale multidimensional array, where each column represents one of the face images of the set (converted from RGB to grayscale and reshaped as a column vector). This restructuring facilitates the application of matrix operations and ensures consistency in the dimensions of the data before PCA is applied. Then, the initial step involves identifying the two components within this set of n -dimensional vectors $P_1 = \{p_{11}, p_{12}, \dots\} \subset \mathbb{R}^n$ that are separated by the maximum distance. This maximum distance represents the longest straight line that can be drawn between two points in the dataset. These two points define the direction of the first principal component.

Once these two points are identified, the second step involves calculating the centroid (mean) of the dataset, which represents the average position of all data points. Then, the direction vector from the centroid to the point furthest away (maximum distance) is considered as the first principal component:

$$\{e_{11}, e_{12}\} = \arg \max_{P_1^i, P_1^j \in P_1} d(p_{1i}, p_{1j}) \quad (7)$$

here, $d(\dots)$ denotes the Euclidean distance.

The first basis vector, v_1 is the vector that connects the two points: $v_1 = e_{11} - e_{12}$. This vector represents the direction of maximum variance between the two furthest points in the dataset, which approximates the first principal component. Typically, to compute the i^{th} basis vector, the process involves projecting the points in the set P_{i-1} onto the hyperplane H_{i-1} . By identifying the two projections with the maximum separation distance, the i^{th} basic vector, v_i is defined as the difference between these two projections, capturing the next most significant direction of variance.

This iterative procedure ensures that each basis vector corresponds to a principal component, providing an efficient approximation of the underlying structure of the dataset. The final outcome is the collection of basis vectors $V = \{v_1, v_2, \dots, v_n\}$, with each vector approximating an eigenface. These eigenfaces form a compact representation of the data, which is useful for tasks such as facial recognition or image compression.

3. IMAGE QUALITY METRICS

Image quality metrics are essential for quantifying the difference or similarity between an original image and a modified version [18]. This paper employs several metrics to assess the disparity between eigenfaces generated by the classical eigenfaces method and our PCA approximation. The evaluation metrics consist of SSIM, MAE, SNR, PSNR, and Euclidean distance.

Considering two images having the same dimensions $M \times N$, $I(i, j)$ represents the initial image, and $K(i, j)$, represents the modified image. Here, i spans from 0 to $M-1$ and j spans from 0 to $N-1$, indicating that each pixel in the image is indexed by its row and column positions. This setup ensures that both images are of identical size, allowing for a pixel-by-pixel comparison between the initial and modified images.

Comparison is often essential in tasks like image processing, where changes at each pixel can be analyzed systematically.

3.1. Mean absolute error

Mean absolute error (MAE) indicates the mean absolute difference between corresponding pixels of an original image and its modified version [19]. It is particularly useful for analyzing uniformly distributed errors across the image. The MAE is calculated as (8):

$$MAE = \frac{1}{MN} \sum_{i=0}^{M-1} \sum_{j=0}^{N-1} |I(i, j) - K(i, j)| \quad (8)$$

MAE offers a simple metric for assessing the average size of discrepancies between the two images, showing how closely the altered image matches the original.

3.2. Mean squared error

Mean squared error (MSE) is applied to calculate the average of the squared intensity differences between two images, which is a fundamental metric used in computing PSNR. MSE is calculated as in (9) [20]:

$$MSE = \frac{1}{MN} \sum_{i=0}^{M-1} \sum_{j=0}^{N-1} |I(i, j) - K(i, j)|^2 \quad (9)$$

MSE is an indicator of the average size of errors between the two images, with higher values signifying larger differences between them.

3.3. Peak signal-to-noise ratio

This metric is employed to assess the squared error between a reference image and a modified image [21], [22]. A higher peak signal-to-noise ratio (PSNR) value indicates greater similarity between the two images, while a lower PSNR value signifies poorer image quality. PSNR is determined through the (10):

$$PSNR_{dB} = 10 \log_{10} \left(\frac{MAX_I^2}{MSE} \right) \quad (10)$$

where MAX_I denotes the highest pixel value in the image, for instance, 255 in the case of 8-bit images. PSNR is expressed in decibels (dB) and provides a standardized measure of image quality, particularly in terms of how much noise or distortion is present relative to the maximum possible intensity of the images.

3.4. Signal-to-noise ratio

Signal-to-noise ratio (SNR) evaluates the proportion of signal power, associated with the restored image, to noise power, which pertains to the discrepancy between the original and degraded images [23]. It is frequently used as a performance metric in image restoration. The formula is:

$$SNR_{dB} = 10 \log_{10} \left[\frac{\sum_{i=0}^{M-1} \sum_{j=0}^{N-1} [I(i, j)]^2}{\sum_{i=0}^{M-1} \sum_{j=0}^{N-1} |I(i, j) - K(i, j)|^2} \right] \quad (11)$$

SNR is expressed in decibels (dB) and quantifies how much stronger the signal (original image) is compared to the noise (distortion) introduced by the modification process. Higher SNR values indicate a better restoration performance, where the restored image closely matches the original image with minimal distortion.

3.5. Structural similarity index measure

The structural similarity index measure (SSIM) metric is a quality metric developed by Li *et al.* [24], designed to assess the similarity of local patterns of pixel intensities in two images X and Y. It comprises three components:

$$Luminance \ l(x, y) = \frac{2\mu_x \mu_y + C_1}{\mu_x^2 + \mu_y^2 + C_1} \quad (12)$$

$$Contrast \ c(x, y) = \frac{2\sigma_x \sigma_y + C_2}{\sigma_x^2 + \sigma_y^2 + C_2} \quad (13)$$

$$\text{Structure } s(x, y) = \frac{\sigma_{xy} + C_3}{\sigma_x \sigma_y + C_2} \quad (14)$$

where μ_x and μ_y are their mean intensities, σ_x and σ_y represent their standard deviations, σ_{xy} denotes the covariance between them, while C_1 , C_2 , and C_3 are constant parameters. Finally, we obtain the SSIM as (15).

$$\text{SSIM}(x, y) = [l(x, y)]^\alpha \cdot [c(x, y)]^\beta \cdot [s(x, y)]^\gamma \quad (15)$$

For $\alpha > 0$, $\beta > 0$ and $\gamma > 0$, these are factors that influence the weight of the three elements. SSIM provides a score between 0 and 1, where 1 indicates perfect similarity between images X and Y.

4. RESULTS AND DISCUSSION

We performed a comparative evaluation between geometrically-approximated eigenfaces and classical eigenfaces using the FEI face database [25]. For this comparison, we employed several image quality metrics: Euclidean distance, MAE, SSIM, SNR, and PSNR. The FEI database includes two types of color face images: 640×480 pixels and 360×260 pixels. Our study focused on the 360×260 pixel images, totaling 200 images.

4.1. Generation of eigenfaces

The initial phase of our comparison involved applying both the eigenfaces method and the geometric approximation of PCA to the FEI database to extract the average face. By comparing the two approaches, we aimed to evaluate how each method captured the essential facial features present in the dataset. Figure 1 illustrates the average faces obtained through both methods, highlighting the differences in the way each technique processes and represents the key components of facial images.



Figure 1. Average faces from the FEI database, average face using eigenfaces method (left panel), average face using approximated eigenfaces (right panel)

Subsequently, we generated all possible eigenfaces using both methods. The number of eigenfaces created matches the count of face images in the database. We specifically chose and analyzed the first 7 eigenfaces obtained via the classical eigenfaces method as shown in Figure 2 and the approximated eigenfaces as shown in Figure 3. These eigenfaces are associated with the largest eigenvalues and thus capture more information from the training images [4].



Figure 2. First 7 eigenface images from the FEI database obtained using the classical eigenfaces



Figure 3. First 7 eigenface images from the FEI database obtained using the approximated eigenfaces

4.2. Quantitative comparison results

We compared the first 7 eigenfaces generated by both methods using image quality metrics. The comparison involved evaluating each pair of eigenfaces based on Euclidean distance, MAE, SNR, PSNR, and SSIM. The metrics were applied to each pair in sequence, starting with the first two eigenfaces, followed by the next two, and so forth.

The data in Table 1 reveal significant differences in image quality metrics between eigenfaces generated by the classical eigenfaces method and the approximated eigenfaces method. The Euclidean distance values are significantly large, indicating considerable discrepancies between eigenfaces produced by the two approaches. MAE values range from 28 to 64, highlighting variances in eigenface representations. SNR values are consistently below 32 dB, reflecting differences in the quality of eigenfaces from both methods. PSNR values, which are negative and below 30 dB, further underscore the variation in eigenface fidelity. Additionally, all SSIM values are below 1, confirming differences in how the two methods capture image structure.

Table 1. Evaluation of eigenfaces derived using both the traditional and approximated eigenfaces techniques

Eigenfaces	Euc distance ($\times 10^3$)	MAE	SNR _{dB}	PSNR _{dB}	SSIM
1	2.3841	28.0314	10.4224	-32.7224	0.1943
2	3.5120	63.4315	1.0533	-39.1457	0.0987
3	3.7018	37.5793	8.4284	-33.7736	0.1153
4	2.7154	54.9430	4.3333	-37.2305	0.0571
5	2.6402	45.0207	4.9677	-36.2332	-0.0910
6	2.7192	42.6299	5.2446	-35.8557	-0.0178
7	3.9907	60.1694	3.0974	-36.8377	-0.0847

These variations primarily result from differences in eigenvector generation. The geometrically-approximated PCA focuses on selecting eigenvectors based on the maximum distances between images, prioritizing geometric properties. In contrast, the classical eigenfaces method derives eigenvectors from covariance matrices, emphasizing statistical relationships. These methodological differences contribute to the observed disparities in eigenface quality and fidelity.

5. CONCLUSION

In this work, we performed a comparative evaluation of the geometrically-approximated PCA method and the classical eigenfaces technique, evaluating their performance using several metrics: Euclidean Distance, PSNR, MAE, SNR, and SSIM. The analysis was performed on the FEI face database, utilizing 200 frontal images for training. Both methods were employed to extract eigenfaces, and the first 7 eigenfaces from each method were assessed.

The results demonstrate notable differences between the two methods. Specifically, the SNR and PSNR values for eigenfaces generated by the geometrically-approximated PCA method were consistently below 30 dB, and the SSIM values were less than 1. These findings indicate a disparity in the quality and fidelity of the eigenfaces produced by the two methods.




The discrepancies observed stem from the differing approaches to eigenvector computation: the geometrically-approximated PCA determines eigenvectors based on the maximum distances between images, while the classical eigenfaces method computes them using covariance matrices. This divergence in methodology has a notable impact on the quality of the resulting eigenfaces, as evidenced by the variations in performance metrics.

Although the geometrically-approximated PCA method provides a more computationally efficient alternative to the classical eigenfaces approach, it may lead to eigenface representations that are less precise. Future research could focus on refining the geometric approximation technique to enhance its accuracy and mitigate the observed differences in performance.




REFERENCES

- [1] K. Karhunen, "About linear methods in probability theory," (in German), *Series A. I. Mathematics-Physics*, vol. 37, pp. 1–79, 1947.
- [2] B. A. De Castro, A. Binotto, J. A. Ardila-Rey, J. R. C. P. Fraga, C. Smith, and A. L. Andreoli, "New algorithm applied to transformers' failures detection based on Karhunen-Loève transform," *IEEE Transactions on Industrial Informatics*, vol. 19, no. 11, pp. 10883–10891, Nov. 2023, doi: 10.1109/TII.2023.3240590.
- [3] H. Chang, C. Wang, Z. Liu, B. Feng, C. Zhan, and X. Cheng, "Research on the Karhunen-Loève transform method and its application to hull form optimization," *Journal of Marine Science and Engineering*, vol. 11, no. 1, p. 230, Jan. 2023, doi: 10.3390/jmse11010230.
- [4] M. Turk and A. Pentland, "Eigenfaces for recognition," *Journal of Cognitive Neuroscience*, vol. 3, no. 1, pp. 71–86, Jan. 1991, doi: 10.1162/jocn.1991.3.1.71.
- [5] L. Guo and S. Wu, "FPGA implementation of a real-time edge detection system based on an improved Canny algorithm," *Applied Sciences*, vol. 13, no. 2, Jan. 2023, doi: 10.3390/app13020870.
- [6] H. ben Fredj, S. Sghair, and C. Souani, "An efficient parallel implementation of face detection system using CUDA," in *2020 5th International Conference on Advanced Technologies for Signal and Image Processing (ATSIP)*, Sep. 2020, vol. 5, pp. 1–6, doi: 10.1109/ATSIP49331.2020.9231723.
- [7] Z. Boubeguir and S. Ghanemi, "GPU-accelerated implementation of Eigenfaces (PCA) algorithm using memory optimization," *Proceedings of the 1st International Conference on Intelligent Systems and Pattern Recognition*, Oct. 2020, pp. 1-5, doi: 10.1145/3432867.3432891.
- [8] A. Baba and T. Bonny, "FPGA-based parallel implementation to classify hyperspectral images by using a convolutional neural network," *Integration*, vol. 92, pp. 15–23, Sep. 2023, doi: 10.1016/j.vlsi.2023.04.003.
- [9] A. Aralikatti, J. Appalla, S. Kushal, G. S. Naveen, S. Lokesh, and B. S. Jayasri, "Real-time object detection and face recognition system to assist the visually impaired," *Journal of Physics: Conference Series*, vol. 1706, no. 1, Dec. 2020, doi: 10.1088/1742-6596/1706/1/012149.
- [10] A. Lorenzon, "Fundamentals of accelerated computing with CUDA C/C++," (in Portuguese) in *Minicursos do XXIII Simpósio em Sistemas Computacionais de Alto Desempenho*, SBC, 2022, pp. 88–105.
- [11] J. Xi, "Analysis of enterprise valuation and future development of Nvidia," *Finance and Economics*, vol. 1, no. 7, Jun. 2024, doi: 10.61173/a4b30582.
- [12] V. Sati, S. M. Sánchez, N. Shoeibi, A. Arora, and J. M. Corchado, "Face detection and recognition, face emotion recognition through nvidia jetson nano," in *Advances in Intelligent Systems and Computing*, vol. 1239, Springer International Publishing, 2021, pp. 177–185.
- [13] N. J. Higham and T. Mary, "Mixed precision algorithms in numerical linear algebra," *Acta Numerica*, vol. 31, pp. 347–414, May 2022, doi: 10.1017/S0962492922000022.
- [14] E. Torti, E. Marenzi, G. Danese, A. J. Plaza, and F. Leporati, "Spatial-spectral feature extraction with local covariance matrix from hyperspectral images through hybrid parallelization," *IEEE Journal of Selected Topics in Applied Earth Observations and Remote Sensing*, vol. 16, pp. 7412–7421, 2023, doi: 10.1109/JSTARS.2023.3301721.
- [15] N. D. F. Atan, R. Rahmadewi, D. Adzani Susanto, and W. Kuncoro Jati, "Implementation of an identification system with facial image processing (Eigenface) using Matlab application," *Jurnal Media Elektrik*, vol. 21, no. 2, pp. 63–72, May 2024, doi: 10.59562/metrik.v21i2.1706.
- [16] F. Ennaama, K. Benhida, and S. Ennaama, "Robust face recognition under advanced occlusion: proposal of an approach based on skin detection and eigenfaces," in *Lecture Notes in Networks and Systems*, vol. 455, Springer International Publishing, 2022, pp. 435–445.
- [17] K. Bartecki, "Classical vs. neural network-based PCA approaches for lossy image compression: Similarities and differences," *Applied Soft Computing*, vol. 161, Aug. 2024, doi: 10.1016/j.asoc.2024.111721.
- [18] Y. Liu, B. Zhang, R. Hu, K. Gu, G. Zhai, and J. Dong, "Underwater image quality assessment: benchmark database and objective method," *IEEE Transactions on Multimedia*, vol. 26, pp. 7734–7747, 2024, doi: 10.1109/TMM.2024.3371218.
- [19] S. Hao and S. Li, "A weighted mean absolute error metric for image quality assessment," in *2020 IEEE International Conference on Visual Communications and Image Processing (VCIP)*, Dec. 2020, vol. 10, pp. 330–333, doi: 10.1109/VCIP49819.2020.9301889.
- [20] B. Girod, "What's wrong with mean squared error?," in *Digital Images and Human Vision*, 1993, pp. 207–220, doi: 10.1109/mdsp.1991.639240.
- [21] Y. Al Najjar, "Comparative analysis of image quality assessment metrics: MSE, PSNR, SSIM, and FSIM," *International Journal of Science and Research (IJSR)*, vol. 13, no. 3, pp. 110–114, Mar. 2024, doi: 10.21275/sr24302013533.
- [22] D. R. I. M. Setiadi, "PSNR vs SSIM: imperceptibility quality assessment for image steganography," *Multimedia Tools and Applications*, vol. 80, no. 6, pp. 8423–8444, Nov. 2021, doi: 10.1007/s11042-020-10035-z.
- [23] K. G. Schilling *et al.*, "Minimal number of sampling directions for robust measures of the spherical mean diffusion weighted signal: Effects of sampling directions, b-value, signal-to-noise ratio, hardware, and fitting strategy," *Magnetic Resonance Imaging*, vol. 94, pp. 25–35, Dec. 2022, doi: 10.1016/j.mri.2022.07.015.
- [24] X. Li, J. Pan, J. Shang, A. Souiri, and M. Gao, "An improved blind/referenceless image spatial quality evaluator algorithm for image quality assessment," *International Journal of Computational Science and Engineering*, vol. 27, no. 1, pp. 48–56, 2024, doi: 10.1504/IJCSE.2024.136250.
- [25] C. E. Thomaz, "FEI face database." *FEI*, 2023. <https://fei.edu.br/~cet/facedatabase.html> (accessed: Aug. 12, 2024).




BIOGRAPHIES OF AUTHORS

Faouzia Ennaama    holds both a master's degree and a doctorate in electrical engineering, focusing on telecommunications and industrial techniques. Her doctoral research, carried out at the LAPSSI laboratory at Cadi Ayyad University in Marrakech, Morocco, led to her earning a Ph.D. in 2020. Her academic and professional journey has been marked by a strong focus on software development, electronics, computer vision, and face recognition. Her proficiency in these areas has resulted in the publication of numerous impactful papers in well-regarded, indexed journals, demonstrating her contributions to advancing both technology and knowledge. Beyond her research accomplishments, Dr. Ennaama is actively involved in the international academic community. She has shared her findings at several global conferences, engaging with peers and presenting innovative solutions to complex challenges. Her commitment to her field is evident through her substantial contributions and recognition by colleagues, reflecting her dedication to pushing the frontiers of technology and research. For academic collaborations or professional inquiries, she can be contacted at email: faouzia.ennaama@ced.uca.ma.



Sara Ennaama    completed her master's degree in business intelligence and big data analytics at Chouaib Doukhali University in 2020, where she gained advanced knowledge in leveraging data for strategic decision-making. Prior to this, she earned her bachelor's degree in mathematical and computer sciences from Cadi Ayyad University, which provided her with a strong foundation in computational theory and applications. Currently, she is pursuing a Ph.D. in computer science at Abdelmalek Essaadi University, focusing on innovative research in computer vision. Her academic journey reflects a deep commitment to understanding and applying cutting-edge technologies to solve complex problems. For professional inquiries or collaborations, she can be contacted at email: sara.ennaama@etu.uae.ac.ma.



Sana Chakri    completed her Ph.D. in software engineering at FSTG - UCA Marrakech and obtained an Engineering degree in software engineering from FST Mohammedia - UH2 Casablanca. Additionally, she also earned a DUT in computer science from FSTG - UCA Marrakech. Her notable work in semantic trajectory knowledge discovery has provided new insights into the behaviors of moving objects and the identification of patterns. By applying her knowledge in data mining, Dr. Chakri links theoretical research with practical solutions, effectively tackling real-world problems. Her commitment to advancing the field of outlier detection not only contributes to the scientific community but also motivates upcoming researchers. Currently, she is focused on developing novel techniques for outlier detection, aiming to enhance understanding and contribute to the advancement of reliable detection frameworks. She can be contacted at email: chakri.sana@gmail.com.